

Contents lists available at ScienceDirect

I.WT

journal homepage: www.elsevier.com/locate/lwt





Utilizing HRPzyme, a cost-effective *Vibrio parahaemolyticus* detection method

Ali Parsaeimehr, Gulnihal Ozbay

Department of Agriculture and Natural Resources, College of Agriculture, Science, and Technology, Delaware State University, Dover, DE, 19901, USA

ARTICLE INFO

Keywords: Colorimetric detection G-quadruplex Crassostrea virginica Callinectes sapidus

ABSTRACT

Vibrio parahaemolyticus is a prominent infectious bacterium responsible for causing widespread cases of acute gastroenteritis in humans globally. In this regard, Colorimetric detection can be essentially used as a sensitive, rapid, and cost-effective detection method. In our research, we have developed a PCR-based detection platform integrated with HRPzyme and utilizing DNAzyme as a signaling probe which mimics peroxidase activity. The colorimetric signal is detectable at concentrations as low as 10^1 cfu mL $^{-1}$ when measured with a spectrophotometer and at 10^3 cfu mL $^{-1}$ through visual inspection. Additionally, extending the polyadenine length to 10 nucleotides resulted in a significant reduction in the background signaling of HRPzyme activity, yielding a relative intensity of 3.07 ± 0.23 arbitrary units (a.u.). Notably, even after a 120-min incubation period, there were no further changes observed in the colorimetric signal in positive samples, maintaining a consistent relative intensity of OD $_{410} = 0.55 \pm 0.08$.

1. Introduction

The world today is increasingly connected in terms of food security, safety, and the outbreak of foodborne illnesses. This issue has been intensified by globalization and the expansion of international food trade. According to the World Health Organization (WHO), an estimated 600 million cases of foodborne illness and 420,000 fatalities occur annually due to the consumption of contaminated food products (WHO, 2022). Among foodborne pathogens, Vibrio parahaemolyticus, a Gram-negative bacterium, significantly contributes to worldwide foodborne morbidity and mortality (Audemard, Ben-Horin, Kator, & Reece, 2022; Cao et al., 2021). This halophilic bacterium is commonly found in marine and estuarine environments across the globe and is frequently isolated from various seafood products. Evidence indicates that V. parahaemolyticus colonizes the human gut and is responsible for acute gastroenteritis when raw or undercooked seafood is consumed. Ensuring the safety of our sea food supplies critically depends on the rapid and accurate detection of V. parahaemolyticus and while traditional culture-based methods are still in use for detecting Vibrio species, they often struggle to accurately identify the isolated species. Consequently, molecular techniques, such as 16S rRNA, ELISA, isotyping, and antisera are gaining popularity to overcome the limitations of culture-based approaches in pathogen detection. In this context, virulence genes (Vir genes) have emerged as crucial molecular markers for pathogen detection. In *V. parahaemolyticus*, numerous *Vir* genes, including *tlh* (thermolabile hemolysin), *tdh* (thermostable direct hemolysin), and *trh* (tdh-related hemolysin), have been identified and sequenced from isolated *V. parahaemolyticus* strains. These genes have been targeted for molecular detection using various clinical and laboratory assays, such as polymerase chain reaction (PCR), reverse transcription–polymerase chain reaction (RT-PCR), and enzyme-linked immunosorbent assay (ELISA) (Paria, Behera, Mohapatra, & Parida, 2021; Alarcón Elvira et al., 2020). Despite their accuracy and efficiency, these techniques are often characterized by high costs, lengthy procedures, complexity, and the use of toxic fluorescence dyes like ethidium bromide. Therefore, there is an urging need for innovative, cost-effective, and eco-friendly approaches to enable large on-site screenings, particularly in resource-poor rural areas (Zhang, He, Feng, & Zhang, 2022).

Recently, a novel approach has been introduced for colorimetric analysis of PCR products. This method involves the addition of horse-radish peroxidase - mimicking DNAzymes (HRPzyme) at the 5' end of the primers. HRPzymes facilitate sequence-specific hybridization, forming G-quadruplex nucleotide sequences that mimic peroxidase activity upon binding to hemin. This mimicry allows for visual detection when the DNAzymes interact with molecules like luminol, 2,2'-azino-bis (3-eth-ylbenzothiazoline-6-sulfonic acid) (ABTS), and 3,3',5,5'-

E-mail address: gozbay@desu.edu (G. Ozbay).

^{*} Corresponding author.

tetramethylbenzidine (TMB) in the presence of hydrogen peroxide (H_2O_2) (Garrido-Maestu et al., 2022). The short HRPzyme sequence (GGGTAGGGCGGGTTGGGT) is designed to allow primer integration in such a way that the functional HRPzyme sequence forms only after the successful amplification of the target genomic region (Ahmad et al., 2021). The HRPzyme-based detection method has demonstrated both specificity and sensitivity, enabling the detection of pathogens like Noroviruses (NoVs) at low concentrations (10 copies per mL). It is effective in detecting various other pathogens, including *Escherichia coli*, *Vibrio parahaemolyticus*, *Listeria monocytogenes*, *Salmonella enterica*, and *Bacillus cereus* (Lee et al., 2022).

In our study, we have successfully established and optimized a colorimetric detection platform. This platform utilizes specific primers targeting the thermolabile hemolysin (tlh) region in V. parahaemolyticus, coupled with the HRPzyme sequence. This innovative technique is characterized by its sensitivity and rapidity, eliminating the need for gel electrophoresis. It can be conveniently employed for on-site detection of V. parahaemolyticus in seafood products, such as Eastern Oyster (Crassostrea virginica) and Blue Crab (Callinectes sapidus).

2. Materials and methods

2.1. Reagents and equipment

We obtained Q5 high-fidelity DNA polymerase (M0491) and a 100-bp ladder (B7025) from New England BioLabs (NEB). All primers used in this study were purchased from Integrated DNA Technologies (Coralville, IA, USA). DNA amplification was conducted using a Bio-Rad thermocycler (T100), and gel electrophoresis was carried out on a 2% w/v agarose gel (Thermo Scientific, 17852) prepared with 1x trisboric acid/EDTA (TAE) buffer. We employed GelRed Nucleic Acid Gel Stain from Biotium, Inc., USA, for DNA staining. In addition to conventional PCR, we employed Real-time PCR (RT-PCR) using Power SYBR Green PCR Master Mix (Applied Biosystems, 4367659) for the molecular detection and confirmation of V. parahaemolyticus. ABTS, Hemin, and hydrogen peroxide (H_2O_2) were purchased from the Sigma-Aldrich (USA), and the Colorimetric assay test was performed using a microplate spectrophotometer device (Bio-Rad, Hercules, CA, USA).

2.2. Microorganisms culture and positive samples selection

V. parahaemolyticus (ATCC 49529, tlh+) was cultured on Thiosulfatecitrate-bile salts-sucrose (TCBS) selective agar (Thermo Scientific. R454752) at 37 °C. The resulting colonies were then molecularly confirmed using specific primers for 16S rRNA and tlh regions. We collected samples using a sterile plastic inoculating loop and resuspended them in 1x phosphate-buffered saline (PBS) to create bacterial suspensions containing 10^0 to 10^7 colony-forming units per milliliter (cfu mL⁻¹). We also conducted a specificity test by comparing V. parahaemolyticus with five other bacterial species. The treatments were carried out in alignment with our prior unpublished study and the findings documented by Lee et al. (2020). These bacteria, namely Klebsiella pneumoniae (ATCC 13883), Escherichia coli (ATCC 43889), Pseudomonas aeruginosa (ATCC 10145), and Staphylococcus aureus (ATCC 14154), were cultured on LB media (Thermo Scientific, 22700025) at 37 °C. However, Shewanella algae (ATCC 51192) was grown on Marin agar (2216E) at 30 °C, and Vibrio cholerae (ATCC 14035) was grown on (TCBS) media at 37 °C. We selected these bacterial species due to their frequent presence in seafood products.

2.3. Primer design and molecular confirmation of the Vibrio parahaemolyticus

We used two sets of primers for the molecular confirmation of *V. parahaemolyticus*: 16S rRNA (F: GGCGTAAAGCGCATGCAGGT, R: GAAATTCTACCCCCCTCTACAG) and *tlh* (F: ACTCAACACAAGAA

GAGATCGACAA; R: GATGAGCGGTTGATGTCCAAA). The PCR were performed under the following conditions: (1) 16S rRNA: denaturation at 95 °C for 3 min, followed by 34 cycles of denaturation at 95 °C for 30 s, annealing at 58 °C for 30 s, and primer extension at 72 °C for 1 min; followed by final extension at 72 °C for 5 min (2) tlh: denaturation at 95 °C for 3 min, followed by 35 cycles of denaturation at 95 °C for 30 s, annealing at 60 °C for 40 s, and primer extension at 72 °C for 1 min; followed by final extension at 72 °C for 10 min (see Fig. 1).

We obtained the sequence data of the *tlh* gene in *V. parahaemolyticus* from the NCBI GeneBank. Using SnapGene software (version 6.0), we designed the forward and reverse primers, which included a protector, HRPzyme sequence, spacer, and the complementary sequence to the targeted region in the *tlh* gene (Supplementary Data Fig. 1). In order to prevent unwanted folding of the HRPzyme sequence (GGG TAGGGCGGGTTGGGT) into a double strand in the presence of Hemin and to minimize background signals, we introduced various lengths of protector sequences (poly A) at the 5' end of both the forward and reverse *tlh* primers. These lengths ranged from 0 to 20 nucleotides, as detailed in Table 1.

In the next stage, we confirmed the amplification of the targeted region using specific HRPzyme-integrated primers through electrophoresis on a 2% agarose gel. To initiate the reaction, we mixed 8 μL of the PCR product with 5 μL of 500 μM hemin dissolved in MES buffer (containing 1% DMSO, 0.05% Triton X-100, 25 mM MES, 200 mM NaCl, 10 mM KCl, pH = 5.1) and allowed it to incubate for 30 min at room temperature. Subsequently, we added 50 μL of 10 mM ABTS, 2 μL of H₂O₂ (30%), and 1 mL of Citrate buffer (pH = 4). The reaction's absorbance was measured at OD = 410 nm.

To optimize the HRPzyme-colorimetric reaction, we explored different primer concentrations (ranging from 15 to 750 nM), annealing temperatures (ranging from 40 to 65 $^{\circ}$ C), and reaction times (ranging from 5 to 60 min). These investigations were conducted using a concentration of 10^4 cfu mL $^{-1}$ of V. parahaemolyticus, and data presented based on 6 independent experiments (replicates = 3).

2.4. Sensitivity and the specificity of the assay for detection of V. parahaemolyticus

We assessed the sensitivity of the colorimetric assay (OD = 410 nm) using a concentration range of V. parahaemolyticus spanning from 10 0 to 10 7 cfu mL $^{-1}$. Subsequently, we compared these results with those obtained from the gel electrophoresis-based assay. We also conducted specificity testing by evaluating the assay's performance against different pathogenic microorganisms, including K. pneumoniae, E. coli, P. aeruginosa, S. aureus, S. algae, Vibrio cholerae, and V. parahaemolyticus. To confirm the results of the colorimetric assay, we also utilized gel electrophoresis (2%).

2.5. Detection of Vibrio parahaemolyticus in Crassostrea virginica and Callinectes sapidus samples

We collected *C. virginica* specimens (n = 10) from one of our monitoring sites located at Latitude 38° 38.613′ N and Longitude 075° 07.631′ W in Rehoboth Beach, Delaware, USA. After collection, the *C. virginica* specimens were thoroughly washed with deionized water. Subsequently, various samples were extracted from the following areas: (1) adductor muscle, (2) heart, (3) pericardial cavity, (4) gonad area, and (5) gill parts. In the subsequent step, we took 100 mg from each of the samples, mixed them, and then subjected the mixture to homogenization and vortexing for 1 min with 1 mL of phosphate buffer (PBS, 1 mM, pH = 7.4), and 100 μ L of the supernatant (centrifuged at 5000 rpm, 2 min) was used for subsequent analysis.

We also collected *C. sapidus* specimens (n=10) from one of our study sites situated at Latitude: 38° 38.613' N and Longitude: 75° 07.55' W in Rehoboth Beach, Delaware, USA. To extract the hemolymph of *C. sapidus*, we used a 1 mL 27 Gauge syringe with a needle.

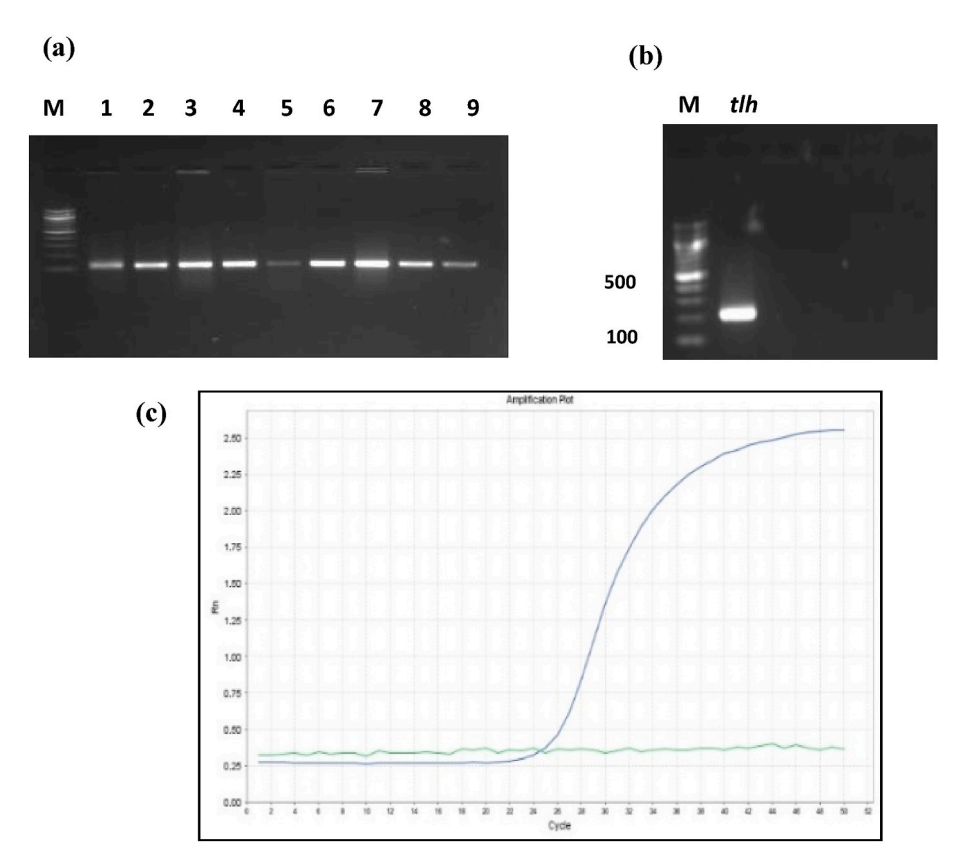


Fig. 1. Molecular confirmation of *Vibrio parahaemolyticus* using specific primers. **(a)** molecular confirmation of *V. parahaemolyticus* using 16s rRNA, **(b)** molecular confirmation of *V. parahaemolyticus* using specific primer for detection of thermolabile hemolysin (*tlh*) gene. **(c)** the confirmation of *V. parahaemolyticus* using RT-PCR. **Note:** The Thiosulfate-Citrate-Bile Salts-Sucrose (TCBS) Agar was used for growth of *V. parahaemolyticus*. The sequence of 16s rRNA primer, F: GGCGTAAAGCGCATGCAGGT, R: GAAATTCTACCCCCCTCTACAG. The sequence of *tlh* primers: F: ACTCAACAAGAAGAGAGATCGACAA; R: GATGAGCGGTT-GATGTCCAAA. PCR condition: 16S rRNA: denaturation at 95 °C for 3 min, followed by 34 cycles of denaturation at 95 °C for 30 s, annealing at 58 °C for 30 s, and primer extension at 72 °C for 1 min; followed by final extension at 72 °C for 10 min.

Table 1Primer's information used for Colorimetric PCR-Based detection of *Vibrio parahaemolyticus* in this study.

Primers Name	Primers sequences (5'-3')				
HRP-Vib-F0	GGGTAGGGCGGTTGGGT <u>AAAAA</u> ACTCAACACAAGAAGAGATCGACAA				
HRP-Vib - R0	GGGTAGGGCGGGTTGGGT <u>AAAAA</u> GATGAGCGGTTGATGTCCAAA				
HRP-Vib- F5	AAAAAGGGTAGGGCGGGTTGGGT <u>AAAAA</u> CTCAACACAAGAAGAGATCGACAA				
HRP-Vib- R5	AAAAAGGGTAGGGCGGGTTGGGT <u>AAAAA</u> GATGAGCGGTTGATGTCCAAA				
HRP-Vib – F10	AAAAAAAAAAAGGGTAGGGCGGGTTGGGTAAAAAAACTCAACACAAGAAGAAGATCGACAA				
HRP- Vib – R10	AAAAAAAAAA				
HRP-Vib – F15	AAAAAAAAAAAAAAAGGGTAGGGCGGGTTGGGTAAAAAACTCAACACAAGAAGAGAGTCGACAA				
HRP-Vib – R15	AAAAAAAAAA				
HRP-Vib – F20 HRP-Vib – R20	AAAAAAAAAAAAAAAAAAAAAAAAAAAAAAAAAAAAAA				

Note: Protector sequences: *Italic*-green colored sequences; HRPzyme sequence: Bold-black colored sequence; spacer: underlined-red colored sequences, specific primer: Blue colored.

Subsequently, 100 mg of the hemolymph was mixed with 100 μ L PBS buffer (1 mM, pH = 7.4), vortexed for 1 min, and the resulting supernatant (obtained after centrifugation at 5000 rpm for 2 min) was utilized for subsequent analysis. We employed a protocol outlined by Rizvi and Bej (2010) to confirm the presence of *V. parahaemolyticus*. This confirmation was achieved using RT-PCR instruments targeting the *tlh* region.

The sizes of the amplicons were subsequently verified by running them on a 2% (w/v) agarose gel alongside a 100-bp ladder. Data presented based on 10 independent experiments (replicates =3).

3. Results and discussion

3.1. Designing an HRPzyme - integrated PCR-based platform for the colorimetric detection of V. parahaemolyticus

Following the lysis of V. parahaemolyticus through boiling (at $100\,^{\circ}\mathrm{C}$ in a water bath for $10\,$ min), we conducted one-step PCR using the designed HRPzyme-integrated primers. Subsequently, we confirmed the PCR amplification through gel electrophoresis. We also examined the design of our HRPzyme-based primers for the formation of primer dimers in non-template samples by visualizing the PCR product on a 2% agarose gel.

According to our design, the HRPzyme sequence present in the primer was blocked during PCR by forming double-stranded DNA. At the end of the PCR, the double-stranded HRPzyme sequence was prevented from folding into a G-quadruplex structure in the presence of hemin. This prevented the HRPzyme from catalyzing the oxidation of ABTS, which is necessary to produce a green-blue color in the presence of hemin and $\rm H_2O_2$.

Additionally, unamplified primers folded in the presence of hemin, leading to the oxidation of ABTS and the production of a green-blue colored product when $\rm H_2O_2$ was added (Fig. 2). As a result, the colorimetric signal inversely correlated with the presence of gene-specific PCR products, being at its maximum in the absence of the target. This enabled us to detect PCR products generated from $\it V. parahaemolyticus$ DNA either through visual observation or by using a UV–visible spectrophotometer."

After incubating the PCR product from the tlh gene with hemin and ABTS, followed by the addition of $\rm H_2O_2$ (30%), we observed a colorimetric signal ranging from dark to light green - blue in the amplified products. Notably, there were no noticeable differences in the colorimetric signal among protector lengths of 0, 5, and 20 nucleotides after an 80-min incubation period. This observation highlights the significant role of protector length in preventing background signals.

Expanding the polyadenine length to 10 nucleotides led to a substantial reduction in the background signaling of HRPzyme activity, resulting in a relative intensity of 3.07 \pm 0.23 arbitrary units (a.u.). This change allowed us to distinguish a light green-blue color compared to other protector lengths. However, increasing the polyadenine length to 20 nucleotides had the opposite effect, resulting in a reduced relative intensity of 1.96 \pm 0.17 a.u. Thus, we selected HRPzyme-integrated primers containing a 10 nt polyadenine sequence as the protector for the subsequent steps of the study (Fig. 2d).

In our experiment, we employed protector and spacer sequences in conjunction with HRPzyme and the complementary sequences designed for the specific targeting of gene sequences. The primary purpose of the protector and spacer sequences was to block the folding of the HRPzyme sequence when it formed a double-stranded configuration, thus it could effectively prevent false-positive reactions. The HRPzyme sequence exhibited peroxidase-like activity by forming a G-quadruplex complex in the presence of hemin. This G-quadruplex complex, originating from the HRPzyme, catalyzed the oxidation of the ABTS substrate in the presence of hydrogen peroxide, resulting in the development of color. In HRPzyme-based detection assays, the length of the protector has consistently been a major concern for researchers seeking to manage background signals generated by HRPzyme sequence activity (Du et al., 2022; Lee et al., 2022).

3.2. Optimization the colorimetric detection of the amplicons

The colorimetric conditions for detecting PCR products were optimized through different experiments involving both negative and positive samples. Colorimetric signals were assessed using both a spectrophotometer and visual observation with the naked eye.

In the initial step, we investigated the impact of annealing temperature (Ta) on the detection of colorimetric signals in our HRPzymeintegrated PCR assay. As shown in Fig. 3 no detectable difference in colorimetric signals were observed between incubation of the positive

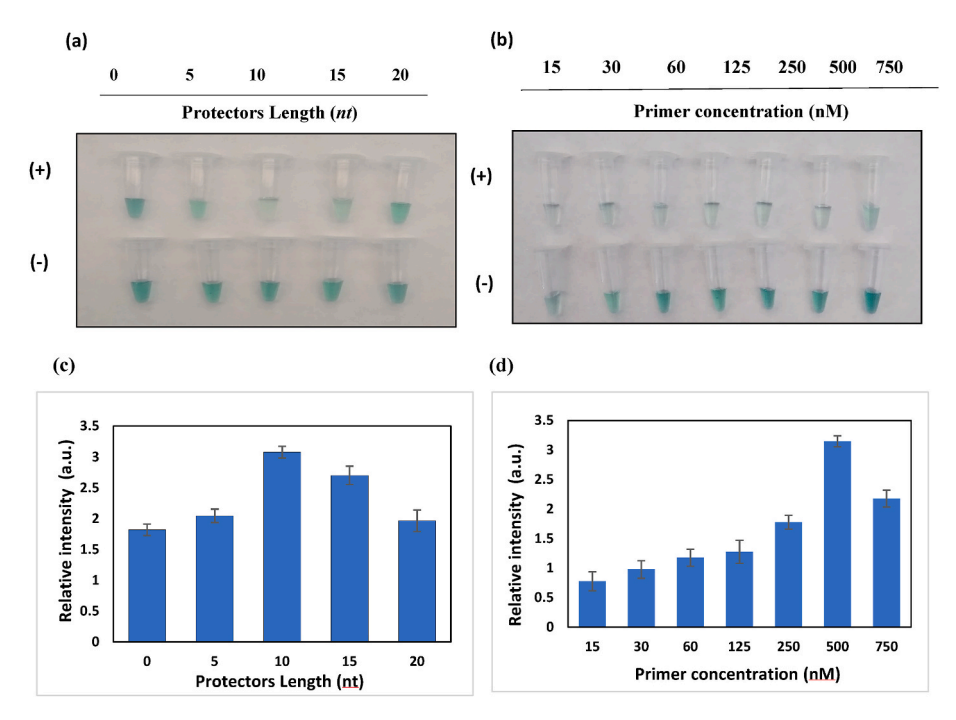


Fig. 2. (a–d). Optimization of the primers used for the sensitive detection of *Vibrio parahaemolyticus* using the colorimetric HRPzyme-integrated PCR assay. (a–b) the influence of primer concentration (nM), (c–d) the influence of protector's length (nt). 10 nt protector length sequence (Relative intensity = 3.07 ± 0.23) was determined as the length for assay. 500 nM was also determined as the best primer concentration (Relative intensity = 3.14 ± 0.31). PCR condition: denaturation at 95 °C for 3 min, incubation time at 60 °C for 30 min, followed by 30 cycles of denaturation at 95 °C for 15 s, annealing at 60 °C for 10 s, and primer extension at 72 °C for 10 s; followed by final extension at 72 °C for 5 min

[Errors bars are representing the standard deviation among 6 different experiments (replicates = 3)].

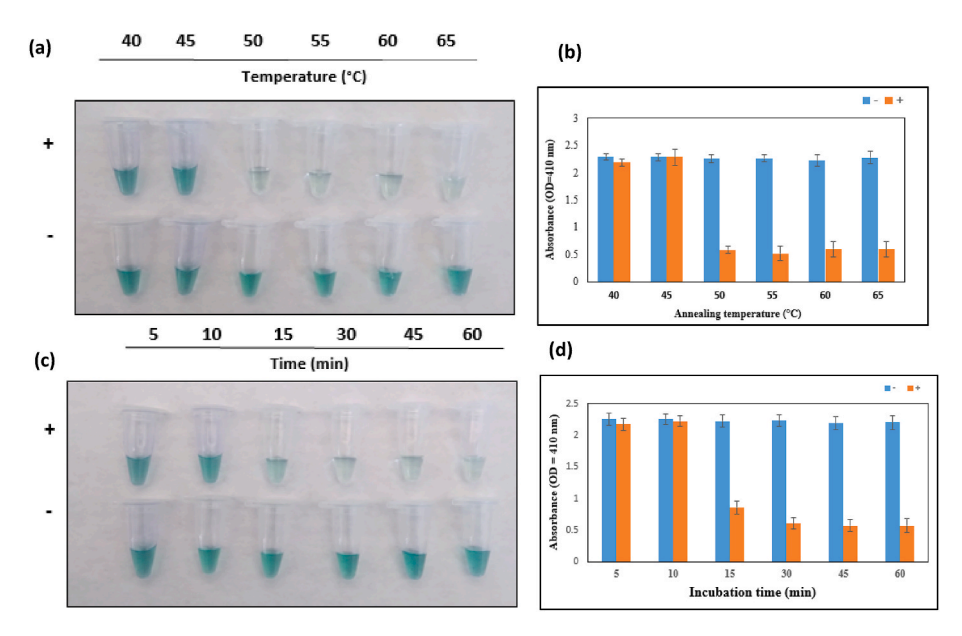


Fig. 3. (a–d). Influence of annealing temperature and incubation time on the Colorimetric HRPzyme-integrated PCR assay for detection of *Vibrio parahaemolyticus* (a) a temperature dependence activity was observed on the colorimetric signal starting at Ta = 50 °C (PCR condition: denaturation at 95 °C for 3 min, incubation time at 60 °C for 30 min, followed by 30 cycles of denaturation at 95 °C for 15 s, annealing at 60 °C for 10 s, and primer extension at 72 °C for 10 s; followed by final extension at 72 °C for 5 min) (b) alternation in colorimetric signals was observed at different denaturation stage using different incubation times (5, 10, 15, 30, 45, 60 min). no difference in colorimetric signal was observed after 30 min incubation time at 60 °C. [Errors bars are representing the standard deviation among 6 different experiments (replicates = 3)].

samples at 40 and 45 °C and the negative samples. However, the signal showed a significant improvement compared to the negative control when we increased the amplification temperature to 65 °C. This indicates that the designed primers were less efficient in binding to the targeted region at lower temperatures (<50 °C), whereas the higher temperature, up to 65 °C, facilitated primer binding, resulting in more reproducible amplification of the targeted region on the tlh gene. We did not detect any significant differences in the colorimetric signals between 60 and 65 °C. Nevertheless, for the subsequent stages of the study, we selected an amplification temperature of 60 °C to prevent the possibility of secondary annealing (Fig. 3). Annealing temperature is a critical step in amplifying the targeted genomic region and addressing the issue of non-specific amplification. During the annealing stage, it is vital to maintain a temperature that allows for the binding of primers to the target DNA. However, it's equally important that, the temperature is not set too low (≤45 °C), as this can lead to the formation of undesired, nonspecific duplexes or intramolecular hairpin structures, both of which can result in false-positive results. Meantime, the higher the temperature is the primer require longer compatible sequence to bind to and as a result your specificity will be higher, since the higher annealing temperatures (>65 °C) possess greater thermal energy and have the potential to interfere with hydrogen bonds, which can hinder primer-template binding. Finding the right balance in annealing temperature is essential for accurate and specific amplification. Various G-quadruplex-based assays have recently been developed for pathogen detection using a range of annealing temperatures, typically from 55 to 65 °C (Achari, Mann, Sharma, & Edwards, 2023; Cao et al., 2022; Huang, Tang, Ismail, & Wang, 2022).

We also found that, the incubation time significantly influences the development of the colorimetric signal. There was no significant difference in the development of the colorimetric signal between 5- and 10-min incubation times for both positive and negative samples (reaction time: 45 min). However, the signal was enhanced when the incubation time was extended to 60 min (OD $_{410}=0.57\pm0.1$). Furthermore, no further alteration in the colorimetric signal in positive samples was observed even after 120 min of incubation (relative intensity = OD $_{410}=0.55\pm0.08$).

The amplification time is a critical parameter that needs to be optimized in G-quadruplex-based assays to ensure accurate and reliable results. The goal of optimization is to strike a balance between achieving sufficient amplification of the target G-quadruplex structure and minimizing the risk of non-specific amplification or primer dimers (DeRosa et al., 2023; Garg, Ahmad, & Kar, 2022). We also examined the impact of different concentrations of HRPzyme-integrated primers (ranging from 15 to 750 nM, with a 10 nt protector length), and observed a concentration-dependent influence on the colorimetric signal when comparing positive and negative samples.

At primer concentrations ranging from 15 to 30 nM, we did not observe a significant signal (indicated by a light green-blue color), which could potentially lead to false colorimetric signals. However, when we increased the primer concentration to 500 nM, we observed a substantial impact on the colorimetric signal in both positive and negative samples.

To ensure the prevention of false-positive results, we utilized a primer concentration of 500 nM, which yielded a relative intensity of 3.08 ± 0.09 a.u. for HRPzyme-integrated primers in the subsequent phases of our study. Prior research has bolded the essential role of primer concentration in modulating the colorimetric signals produced by G-quadruplex DNAzymes. Distinguishing between the colorimetric signals of negative and positive samples becomes challenging at lower concentrations of HRPzyme-integrated primers. Conversely, higher primer concentrations may introduce an excess of free primers, potentially leading to false-positive color development (Hanyue et al., 2023; Lee et al., 2022).

3.3. The sensitivity and specificity of the PCR-based platform integrated with HRPzyme for colorimetric detection of V. parahaemolyticus

We employed the following optimized amplification conditions for assessing the sensitivity and specificity of the introduced HRPzymeintegrated PCR platform for the detection of V. parahaemolyticus: denaturation at 95 °C for 3 min, an incubation period at 60 °C for 30 min, followed by 30 cycles of denaturation at 95 °C for 15 s, annealing at 60 °C for 10 s, and primer extension at 72 °C for 10 s, concluding with a

final extension step at 72 $^{\circ}$ C for 5 min. To evaluate the sensitivity of the assay, a series of *V. parahaemolyticus* dilutions (ranging from 0 to 10^7 cfu mL $^{-1}$) were prepared in 1x PBS buffer.

The amplification of the targeted *tlh* gene region was carried out using a PCR thermocycler, and the success of the PCR amplification was confirmed through agarose gel electrophoresis to eliminate the possibility of false-positive signals. As illustrated in Fig. 4, the band intensities observed in the gel electrophoresis directly correlated with the concentration of *V. parahaemolyticus*. Additionally, the colorimetric signals displayed an inverse relationship with the concentration of the tested *V. parahaemolyticus*, allowing for clear differentiation from the negative control.

The linear relationship between various concentrations of V. parahaemolyticus and the optical density (OD = 410) showed a strong correlation ($R^2=0.98$). Our findings indicate that, the colorimetric signals were inversely proportional to the concentration of the tested V. parahaemolyticus, allowing for clear differentiation from the negative control. Notably, even at lower concentrations, the colorimetric signal was detectable using a spectrophotometer, becoming visible at a concentration as low as 10^3 cfu mL $^{-1}$ (OD₄₁₀: 1.3 ± 0.2).

In the specificity test, a variety of pathogens, including *K. pneumoniae*, *E. Coli*, *P. aeruginosa*, *S. aureus*, *S. algae*, and *V. cholerae* were examined alongside *V. parahaemolyticus* using the optimized HRPzyme-integrated PCR assay. These pathogens were chosen due to their common occurrence in seafood products. To provide an additional layer of confirmation, the PCR products were subjected to gel electrophoresis, allowing for a comparison between the colorimetric signals obtained and the positive bands generated.

As illustrated in Fig. 5, among the array of pathogens examined, a positive colorimetric signal was exclusively detected for V. parahaemolyticus (OD $_{410}$: 0.4 \pm 0.03). This outcome was subsequently validated through both PCR and RT-PCR, as shown in Fig. 5. These results unequivocally establish the remarkable specificity of the HRPzyme-integrated PCR assay, specifically designed for the precise detection of the target pathogen.

G-quadruplex-based assays and PCR techniques are frequently utilized for pathogen detection, with a substantial body of evidence indicating that G-quadruplex-based assays offer high sensitivity and specificity. A recent Meta-Analysis on the available reports shows the PCR and G-quadruplex based assays has the sensitivity 95.6% and 96.6% and specificity of 98.7% and 97.6%, respectively (Sadeghi et al., 2021).

Our results also demonstrate that, the proposed assay exhibits a sensitivity comparable to the PCR approach. The colorimetric signal can be detected at a concentration as low as 10^1 cfu mL $^{-1}$ using a spectro-photometer and at 10^3 cfu mL $^{-1}$ by the naked eye. However, when the test results fall within a range lower than 10^3 CFU mL $^{-1}$, the positive identification outcomes using the HRPzyme-integrated PCR-based

platform are diminished. Therefore, we recommend the use of culturebased methods for *V. parahaemolyticus* identification as a complementary approach.

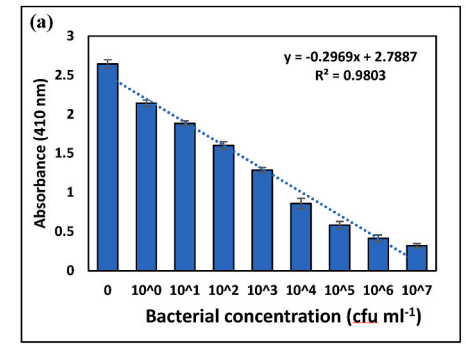
3.4. Validation of the HRPzyme-integrated PCR-based colorimetric platform for the detection of V. parahaemolyticus in C. virginica and C. sanidus

To evaluate the applicability and reliability of our test, we applied our proposed HRPzyme-integrated PCR-based platform to detect *V. parahaemolyticus* in Eastern oysters (*C. virginica*) and blue crabs (*C. sapidus*). In this context, various samples were gathered from the muscle, heart, pericardial cavity, gonad area, and gills of the *C. virginica*. Positive colorimetric signals were then compared to the outcomes obtained through gel electrophoresis and the RT-PCR method.

As illustrated in Fig. 6, a distinct colorimetric signal ($OD_{410}=0.43\pm0.02$) was evident in the organs tested, indicating contamination with V. parahaemolyticus in the C. virginica samples. These findings were further validated through PCR and RT-PCR. Notably, no amplified bands were observed in the negative agarose gel electrophoresis of the V. parahaemolyticus samples, whereas a specific band of the correct size was consistently obtained in the gel electrophoresis results.

To assess the test's validity in *C. sapidus*, hemolymph from both *V. parahaemolyticus*-positive and -negative samples was extracted and compared. As depicted in Fig. 7, the colorimetric signal generated by our proposed HRPzyme-integrated PCR-based platform was distinctly observed in the *V. parahaemolyticus*-positive samples ($OD_{410}=0.5\pm0.03$). These results were consistently supported by gel electrophoresis and RT-PCR analysis, providing parallel confirmation. These findings strongly endorse the specificity of the HRPzyme-integrated PCR assay for detecting the targeted pathogen, enabling the identification of *V. parahaemolyticus* in seafood products. The assay's specificity relies on the precise primers integrated with HRPzyme for the targeted *tlh* sequence, enabling the detection of this specific foodborne pathogen.

Owing to diverse impacts of the food products on the public health, the safety of the food products must be the main concern during the harvesting phase. In this regard, there is an essential need for accurate, sensitive, fast, and straightforward molecular biology-based techniques to detect the pathogens however the specificity of the primers will play the major role, for example RdRP and BPO genes were employed for detection of different genogroup of noroviruses (Lee et al., 2022), ORF-1ab and N-gene were used for detection of SARS-CoV-2 (Ahmad et al., 2021) and here by this study we suggest targeting specific region on tlh gene for detection of V. parahaemolyticus using the HRPzyme-integrated PCR assay. Compared to other available methods, such as gold nanoparticle-based enzyme-linked antibody, magnetic nanoparticles, CE–RAA–CRISPR assay, and Duplex droplet digital PCR,



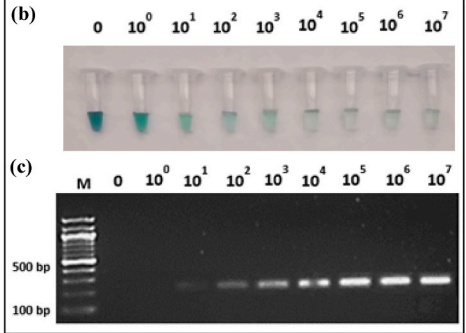


Fig. 4. (a–c). Colorimetric HRPzyme-integrated PCR assay results of *Vibrio parahaemolyticus* in our study. (a) gel electrophoresis data of different concentration of *V. parahaemolyticus*, (b) colorimetric HRPzyme-integrated PCR results of different concentration of *V. parahaemolyticus*, (c) absorbance data of colorimetric HRPzyme-integrated PCR assay at different concentration of bacteria. PCR condition: denaturation at 95 °C for 3 min, incubation time at 60 °C for 30 min, followed by 30 cycles of denaturation at 95 °C for 15 s, annealing at 60 °C for 10 s, and primer extension at 72 °C for 10 s; followed by final extension at 72 °C for 5 min [Errors bars are representing the standard deviation among 6 different experiments (replicates = 3)].

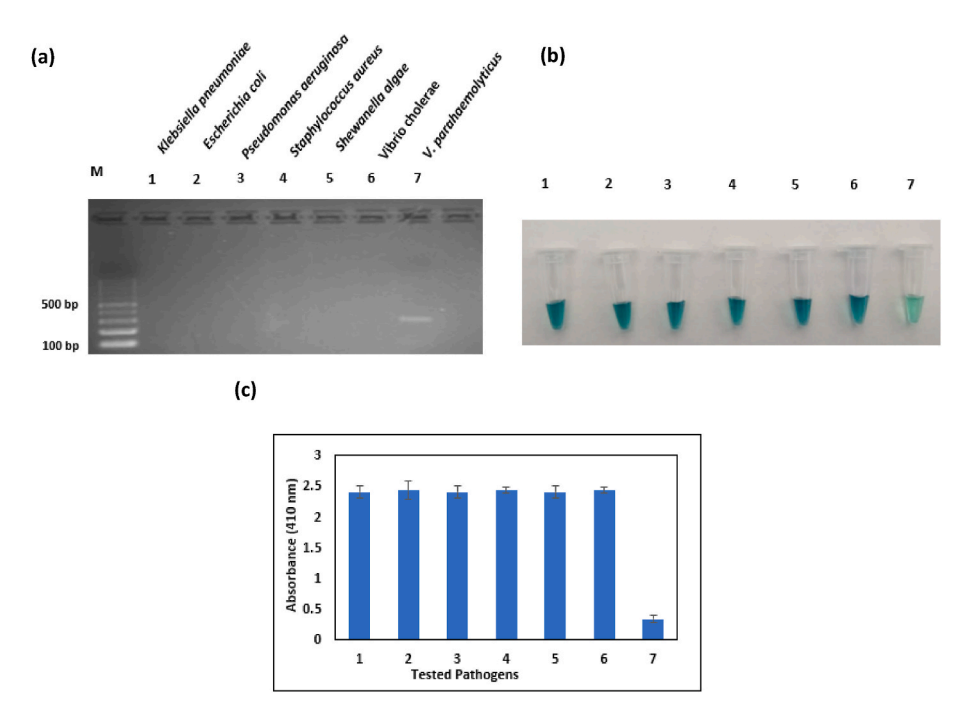


Fig. 5. (a–c) Specificity test of Colorimetric HRPzyme-integrated PCR assay results of *Vibrio parahaemolyticus*. (a) gel electrophoresis data on the specificity test of *V. parahaemolyticus* against tested pathogens, (b) colorimetric HRPzyme-integrated PCR results (c) absorbance data of colorimetric HRPzyme-integrated PCR assay. Errors bars are representing the standard deviation among 6 different experiments. Colorimetric PCR-based detection method. Note: the samples were run at $60\,^{\circ}$ C for a duration of $60\,^{\circ}$ min and read at the OD = $410\,^{\circ}$ nm. $100\,^{\circ}$ bp ladder was used for molecular confirmation.

[Data is presenting based on $10\,^{\circ}$ independent experiments, replicates = 3].

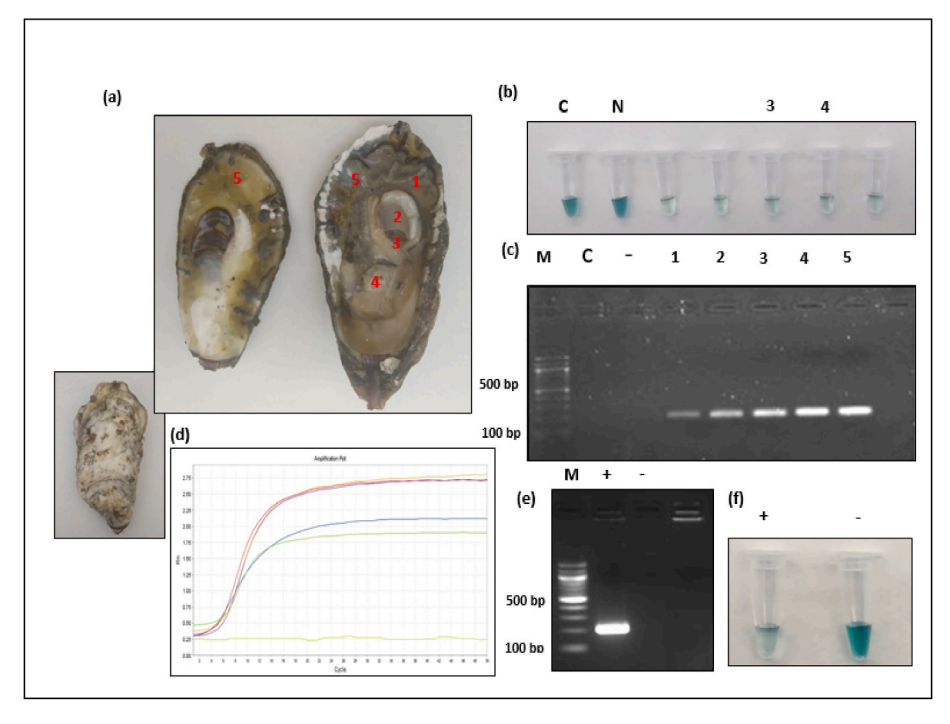


Fig. 6. (a–c) Colorimetric HRPzyme-integrated PCR assay results of *Vibrio parahaemolyticus* on Oyster. (a) Oyster, (b, f) colorimetric HRPzyme-integrated PCR results of different concentration of *V. parahaemolyticus*, (c, e) molecular confirmation on the presence of the *V. parahaemolyticus* using gel electrophoresis data of different concentration of *V. parahaemolyticus* (d) the RT-PCR confirmation on the presence of the *V. parahaemolyticus*. Note: (1) adductor muscle, (2) heart, (3) pericardial cavity, (4) gonad area, and (5) the gills parts.

[Data is presenting based on 10 independent experiments, replicates = 3].

our proposed method has the potential to be both faster and more cost-effective (Table 2). However, it's essential to keep in consideration that, the quantity of targeted DNA can change significantly among

different samples. This variety presents a notable challenge when attempting to establish uniform diagnostic performance criteria, particularly with specific sample types. Additionally, distinguishing

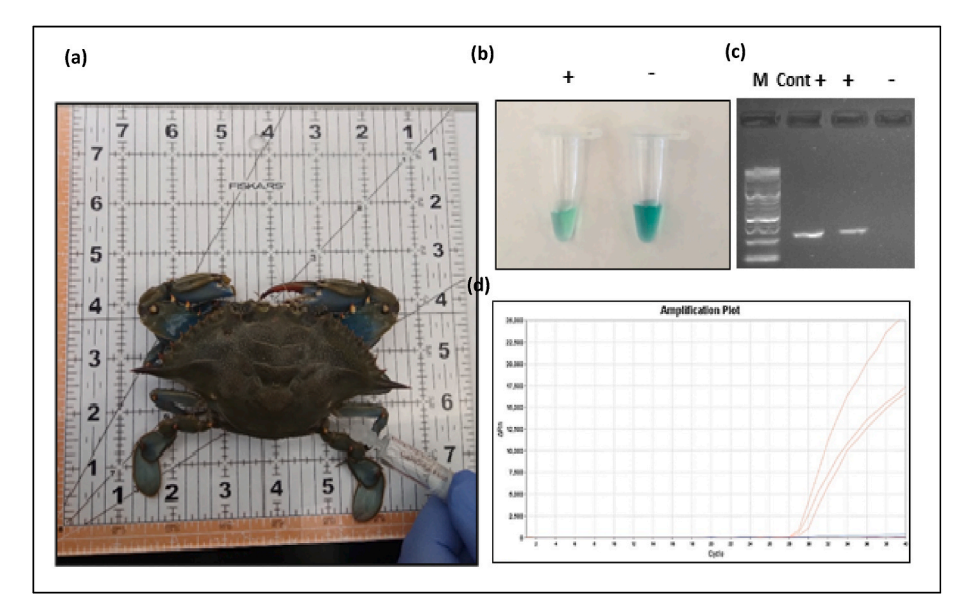


Fig. 7. (a–d) Colorimetric HRPzyme-integrated PCR assay results of *Vibrio parahaemolyticus* on Blue Crab. (a) isolating hemolymph from the Blue crab, (b, f) colorimetric HRPzyme-integrated PCR results of different concentration of *V. parahaemolyticus*, (c, e) molecular confirmation on the presence of the *V. parahaemolyticus* using gel electrophoresis data of different concentration of *V. parahaemolyticus* (d) the RT-PCR confirmation on the presence of the *V. parahaemolyticus*.

[Data is presenting based on 10 independent experiments, replicates = 3].

Table 2Comparison of the developed HRPzyme-Based *Vibrio parahaemolyticus*. detection with Other Methods.

	Method	Detection time	Detection range	Characteristics	References
		(h)	(cfu ml ⁻¹)		
1	Streak Plate/probe method	<72	10 ⁵ -10 ⁰	Lengthy and	Blackstone et al. (2003)
				costly	
2	Real time PCR method	<4	$10^5 - 10^0$	Lengthy and	Costa, Ferreira, Simões, Silva, and
				costly	Campos (2022)
3	PCR based	<2	$10^5 - 10^0$	Costly	Bonny et al. (2022)
4	Gold nanoparticle-based enzyme-linked antibody	<3	$10^3 - 10^0$	Lengthy and	Wu et al. (2014)
				costly	
5	Magnetic nanoparticles	<12	10^1	Lengthy and	Blank-Shim et al. (2017)
				costly	
6	CE-RAA-CRISPR Assay	<5	6.7×10^1	Lengthy and	Lv et al. (2022)
				costly	
7	Visual Detection of V. parahaemolyticus using Combined CRISPR/Cas12a and	30 min	10^{2}	Costly	Jiang et al. (2022)
	Recombinase Polymerase Amplification				
8	Duplex droplet digital PCR combined with propidium monoazide	30 min	8.15×10^{1}	Costly	Zhou et al. (2023)
9	HRPzyme based targeting <i>tlh</i> region	2	10^{3}	Rapid and cheap	This study

between active infection and asymptomatic colonization poses a challenge when using the HRPzyme-integrated PCR-based platform because the method does not differentiate between live and dead cells. Hence, it is essential to take these limitations into account when using this method as a diagnostic tool and to employ a complementary approach as needed (Vuong et al., 2022).

4. Conclusion

The global consumption of seafood products has witnessed a significant increase, emphasizing the critical importance of promptly detecting pathogens like *V. parahaemolyticus*. Thus, accurate, rapid and straight forward methods for high-through put screening of pathogens is a necessary demand. In this study, we have introduced a HRPzymeintegrated PCR based platform for colorimetric detection of *V. parahaemolyticus* targeting a specific region on the *tlh* gene to form G-quadruplex DNAzymes. In this study, we utilized the G-quadruplex loop region to create a binding site for hemin, resulting in the formation of a

catalytic G-quadruplex/hemin DNAzyme. The catalytic cycle of this DNAzyme is initiated by the peroxidase enzyme, and the colorimetric HRPzyme-integrated PCR detection platform was optimized with 500 nM forward and reversed primers and ${\bf Ta}$ of 60 $^{\circ}{\rm C}$ and reaction time of 60 min.

The method may detect the V. parahaemolyticus at the concentration of 10 cfu $\rm mL^{-3}$ by naked-eye and can be accomplished within 2 h. In contrast to the existing PCR and RT-PCR techniques our approach showed several advantages such as rapid V. parahaemolyticus detection, increase cost effectiveness, and being eco-friendly by eliminating the usage of toxic fluorescence dyes, such as ethidium bromide.

CRediT authorship contribution statement

Ali Parsaeimehr: designed and carried out the experiments, analyzed the data, wrote the manuscript, revised and edited the manuscript. Gulnihal Ozbay: revised and edited the manuscript.

Declaration of competing interest

The authors declare that they have no known competing financial interests or personal relationships that could have appeared to influence the work reported in this paper.

Data availability

Data will be made available on request.

Acknowledgements

This project is funded by NSF EPSCOR WICCED Program Grant No. 1757353 and the State of Delaware.

Appendix A. Supplementary data

Supplementary data to this article can be found online at https://doi.org/10.1016/j.lwt.2023.115461.

References

- Achari, S. R., Mann, R. C., Sharma, M., & Edwards, J. (2023). Diagnosis of Fusarium oxysporum f. sp. ciceris causing Fusarium wilt of chickpea using loop-mediated isothermal amplification (LAMP) and conventional end-point PCR. Scientific Reports, 13, Article 2640. https://doi.org/10.1038/s41598-023-29730-6
- Ahmad, M., Sharma, P., Kamai, A., Agrawal, A., Faruq, M., & Kulshreshtha, A. (2021). HRPZyme assisted recognition of SARS-CoV-2 infection by optical measurement (HARIOM). Biosensors and Bioelectronics, 187, Article 113280. https://doi.org/ 10.1016/j.bios.2021.113280
- Alarcón Elvira, F., Pardío Sedas, V. T., Martínez Herrera, D., Quintana Castro, R., Oliart Ros, R. M., López Hernández, K., et al. (2020). Comparative survival and the coldinduced gene expression of pathogenic and nonpathogenic Vibrio parahaemolyticus from tropical eastern oysters during cold storage. International Journal of Environmental Research and Public Health, 17, Article 1836.
- Audemard, C., Ben-Horin, T., Kator, H. I., & Reece, K. S. (2022). Vibrio vulnificus and Vibrio parahaemolyticus in oysters under low tidal range conditions: Is seawater analysis useful for risk assessment? Foods, 11, Article 4065. https://doi.org/ 10.3390/foods11244065
- Blackstone, G. M., Nordstrom, J. L., Vickery, M. C., Bowen, M. D., Meyer, R. F., & DePaola, A. (2003). Detection of pathogenic Vibrio parahaemolyticus in oyster enrichments by real time PCR. Journal of Microbiological Methods, 53, 149–155. https://doi.org/10.1016/S0167-7012(03)00020-4
- Blank-Shim, S. A., Schwaminger, S. P., Borkowska-Panek, M., Anand, P., Yamin, P., Fraga-García, P., et al. (2017). Binding patterns of homo-peptides on bare magnetic nanoparticles: Insights into environmental dependence. *Scientific Reports*, 7, Article 14047. https://doi.org/10.1038/s41598-017-13928-6
- Bonny, S. Q., Hossain, M. M., Uddin, S. M. K., Pulingam, T., Sagadevan, S., & Johan, M. R. (2022). Current trends in polymerase chain reaction-based detection of three major human pathogenic vibrios. *Critical Reviews in Food Science and Nutrition*, 62, 1317–1335. https://doi.org/10.1080/10408398.2020.1841728
- 62, 1317–1335. https://doi.org/10.1080/10408398.2020.1841728
 Cao, J., Liu, H., Wang, Y., He, X., Jiang, H., Yao, J., et al. (2021). Antimicrobial and antivirulence efficacies of citral against foodborne pathogen Vibrio parahaemolyticus RIMD2210633. Food Control, 120, Article 107507. https://doi.org/10.1016/j.foodcont.2020.107507
- Cao, Y., Ye, C., Zhang, C., Zhang, G., Hu, H., Zhang, Z., et al. (2022). Simultaneous detection of multiple foodborne bacteria by loop-mediated isothermal amplification on a microfluidic chip through colorimetric and fluorescent assay. Food Control, 134, Article 108694. https://doi.org/10.1016/j.foodcont.2021.108694
- Costa, C., Ferreira, G. D., Simões, M., Silva, J. L., & Campos, M. J. (2022). Real-time PCR protocol for detection and quantification of three pathogenic members of the Vibrionaceae family. *Microorganisms*, 10, Article 2060. https://doi.org/10.3390/microorganisms10102060
- DeRosa, M. C., Lin, A., Mallikaratchy, P., McConnell, E. M., McKeague, M., Patel, R., et al. (2023). In vitro selection of aptamers and their applications. *Nature Nat Rev Methods Primers*, 3, Article 54. https://doi.org/10.1038/s43586-023-00238-7

- Du, R., Yang, X., Jin, P., Guo, Y., Cheng, Y., Yu, H., et al. (2022). G-quadruplex based biosensors for the detection of food contaminants. Critical Reviews in Food Science and Nutrition, 1–15. https://doi.org/10.1080/10408398.2022.2059753
- Garg, N., Ahmad, F. J., & Kar, S. (2022). Recent advances in loop-mediated isothermal amplification (LAMP) for rapid and efficient detection of pathogens. Current Research in Microbial Sciences., Article 100120. https://doi.org/10.1016/j. cepsigr. 2022.100120.
- Garrido Maestu, A., & Prado, M. (2022). Naked-eye detection strategies coupled with isothermal nucleic acid amplification techniques for the detection of human pathogens. Comprehensive Reviews in Food Science and Food Safety, 21, 1913–1939. https://doi.org/10.1111/1541-4337.12902
- Hanyue, X., Yanjin, F., Shihui, W., Yao, L., Xiong, X., & Ying, Y. (2023). Closed-tube visual detection of Atlantic cod (*Gadus morhua*) using self-quenched primer coupled with a designed loop-mediated isothermal amplification vessel. *Journal of the Science of Food and Agriculture*, 103, 6025–6032. https://doi.org/10.3390/ijerph17061836
- Huang, X., Tang, G., Ismail, N., & Wang, X. (2022). Developing RT-LAMP assays for rapid diagnosis of SARS-CoV-2 in saliva. EBioMedicine, 75, Article 103736. https://doi. org/10.1016/j.ebiom.2021.103736
- Jiang, H. J., Rong, T. A. N., Min, J. I. N., Jing, Y. I. N., Gao, Z. X., Li, H. B., et al. (2022). Visual detection of Vibrio parahaemolyticus using combined CRISPR/Cas12a and recombinase polymerase amplification. Biomedical and Environmental Sciences, 35, 518–527. https://doi.org/10.3967/bes2022.069
- Lee, J. E., Kim, S. A., Park, H. J., Mun, H., Ha, K. S., & Shim, W. B. (2022). Colorimetric detection of norovirus by helicase-dependent amplification method based on specific primers integrated with HRPzyme. *Analytical and Bioanalytical Chemistry*, 414, 6723–6733. https://doi.org/10.1007/s00216-022-04247-5
- Lee, J. E., Mun, H., Kim, S. R., Kim, M. G., Chang, J. Y., & Shim, W. B. (2020). A colorimetric Loop-mediated isothermal amplification (LAMP) assay based on HRP-mimicking molecular beacon for the rapid detection of Vibrio parahaemolyticus. Biosensors and Bioelectronics, 151, Article 111968. https://doi.org/10.1016/j.bios.2019.111968
- Lv, X., Cao, W., Zhang, H., Zhang, Y., Shi, L., & Ye, L. (2022). CE-RAA-CRISPR assay: A rapid and sensitive method for detecting Vibrio parahaemolyticus in seafood. Foods, 11, Article 1681. https://doi.org/10.3390/foods11121681
- Paria, P., Behera, B. K., Mohapatra, P. K. D., & Parida, P. K. (2021). Virulence factor genes and comparative pathogenicity study of tdh, trh and tlh positive *Vibrio* parahaemolyticus strains isolated from Whiteleg shrimp, Litopenaeus vannamei (Boone, 1931) in India. *Infection, Genetics and Evolution, 95*, Article 105083. https:// doi.org/10.1016/j.meegid.2021.105083
- Rizvi, A. V., & Bej, A. K. (2010). Multiplexed real-time PCR amplification of tlh, tdh and trh genes in Vibrio parahaemolyticus and its rapid detection in shellfish and Gulf of Mexico water. Antonie van Leeuwenhoek, 98, 279–290. https://doi.org/10.1007/ s10482-010-9436-2
- Sadeghi, Y., Kananizadeh, P., Moghadam, S. O., Alizadeh, A., Pourmand, M. R., Mohammadi, N., et al. (2021). The sensitivity and specificity of loop-mediated isothermal amplification and PCR methods in detection of foodborne microorganisms: A systematic review and meta-analysis. *Iranian Journal of Public Health*, 50, Article 2172. https://doi:10.18502/ijph.v50i11.7571.
- Vuong, L. N., Dorsey, D., Obernuefemann, C., Pinkner, J., Walker, J. N., Hultgren, S., et al. (2022). Characterization of host-pathogen-device interactions in Pseudomonas aeruginosa infection of breast implants. *Plastic and Reconstructive Surgery*, 150, 260e–271e. https://doi.org/10.1097/PRS.0000000000000315
- World Health Organization. (2022). WHO global strategy for food safety 2022-2030: Towards stronger food safety systems and global cooperation.
- Wu, W., Li, J., Pan, D., Li, J., Song, S., Rong, M., et al. (2014). Gold nanoparticle-based enzyme-linked antibody-aptamer sandwich assay for detection of Salmonella Typhimurium. ACS Applied Materials & Interfaces, 6, 16974–16981. https://doi.org/ 10.1021/am5045828
- Zhang, W., He, Y., Feng, Z., & Zhang, J. (2022). Recent advances of functional nucleic acid-based sensors for point-of-care detection of SARS-CoV-2. *Microchimica Acta*, 189, 1–18. https://doi.org/10.1007/s00604-022-05242-4
- Zhou, H., Liu, X., Lu, Z., Hu, A., Ma, W., Shi, C., et al. (2023). Quantitative detection of Vibrio parahaemolyticus in aquatic products by duplex droplet digital PCR combined with propidium monoazide. *Food Control*, 144, Article 109353. https://doi.org/ 10.1016/j.foodcont.2022.109353

Further reading

Wang, D. G., Brewster, J. D., Paul, M., & Tomasula, P. M. (2015). Two methods for increased specificity and sensitivity in loop-mediated isothermal amplification. *Molecules*, 20, 6048–6059. https://doi.org/10.3390/molecules20046048